Molecular Conformation and Melting Behavior of Alkyl/Oligo(oxyethylene)/Alkyl Triblock Position Isomers: Effect of the Position of an Oligo(oxyethylene) Block

Koichi Fukuhara,* Hirotaka Kumamoto, and Hiroatsu Matsuura

Department of Chemistry, Graduate School of Science, Hiroshima University, Kagamiyama, Higashi-Hiroshima 739-8526, Japan

Received: March 14, 2006; In Final Form: June 19, 2006

The molecular conformation and melting behavior of triblock position isomers $H(CH_2)_k(OCH_2CH_2)_4O(CH_2)_{12-k}H$ (abbreviated as $C_kE_4C_{12-k}$) with $k = 6-11$ have been studied by infrared spectroscopy and differential scanning calorimetry (DSC), with focus on the effect of the position of an oligo(oxyethylene) block in the molecule. The analysis of infrared spectra has revealed that the stable molecular form changes from a fully planar structure (γ form) to a planar/helical/planar structure (β form) with a change of the position of the tetrakis(oxyethylene) block from the center to the end of the molecule. The DSC measurements have shown that the melting points of the γ-form solid decrease and the melting points of the β-form solid increase with a shift of the tetrakis(oxyethylene) block toward the terminal of the molecule. The stabilities of the two molecular forms change over between $k = 8$ and 9. $C_8E_4C_4$ and $C_9E_4C_3$ exhibit contrasting conformational behavior with temperature; when the temperature is increased, the metastable β form of $C_8E_4C_4$ transforms into the stable γ form, while the metastable γ form of $C_9E_4C_3$ transforms into the stable β form. The metastable γ form with a planar oligo(oxyethylene) block is a new finding in the present work. The experimental results of the stabilities of molecular forms are explained by the relative stabilities of partial crystal lattices formed by the alkyl and oligo(oxyethylene) blocks.

Introduction

Crystalline block copolymers have attracted increasing attention in the field of nanotechnology because of the diverse structures and morphologies of microdomains involved in the crystalline blocks.[1−3] Block copolymers consisting of alkyl and oligo(oxyethylene) blocks are the most adequate compounds for investigating the microdomain structures and their correlations with physical properties, because the component blocks have high crystallizability and stereoregularity, and the lengths of the blocks are controllable. The intrinsic conformational form of the alkyl chain is an extended zigzag structure with an all-trans conformation,[4] while that of the oligo(oxyethylene) chain is a helical structure with repeated trans−gauche−trans conformations for the $O-CH_2-CH_2-O$ segments.[5]

Booth and co-workers have studied the thermal properties and crystal structures of alkyl/oligo(oxyethylene)/alkyl triblock compounds $H(CH_2)_n(OCH_2CH_2)_mO(CH_2)_nH$ (abbreviated as $C_nE_mC_n$) with $n = 1-26$ and $m = 9$ and 15 by using various experimental methods that include differential scanning calorimetry (DSC), X-ray diffraction, and infrared and Raman spectroscopy.[6−11] They have found several structures of the solids and classified them into three types on the basis of the crystallinity of the component blocks.

We have studied the molecular structures of short-chain symmetric $C_nE_mC_n$ compounds with $n = 3-10$ and $m = 1-8$[12−15] and asymmetric $C_8E_4C_n$ compounds with $n = 2-7$,[16] and identified two distinctive molecular forms in the solid state: one, called the γ form, with a fully planar structure and the other, called the β form or the $\alpha\beta$ form, with a planar/helical/planar triblock structure. We have shown by examining the results on a number of $C_nE_mC_{n'}$s ($n = n'$ or $n \neq n'$) that the molecular form depends primarily on the relative lengths of the component blocks. Namely, the molecules assume the fully planar γ form in cases where the number of backbone atoms in the end alkyl blocks is larger than or comparable to that in the central oligo(oxyethylene) block. In other cases, the molecules assume a planar/helical/planar form such as the β form or the $\alpha\beta$ form. It is noteworthy that, contrary to the above trend of preferred molecular conformations, the methoxy-terminated $C_{16}E_4C_1$ adopts a molecular form that contains a helix of the oligo(oxyethylene) chain,[17] even though the number of backbone atoms in the alkyl block is larger than that in the oligo(oxyethylene) block. This consequence strongly suggests that the position of the oligo(oxyethylene) block in the molecule can also be a substantial factor that determines the molecular form.

In this work, we study the effect of the position of an oligo(oxyethylene) block in the $C_nE_mC_{n'}$ molecule on the conformation and melting behavior. The compounds studied are six position isomers $H(CH_2)_k(OCH_2CH_2)_4O(CH_2)_{12-k}H$ (abbreviated as $C_kE_4C_{12-k}$) with $k = 6-11$, that is, $C_6E_4C_6$, $C_7E_4C_5$, $C_8E_4C_4$, $C_9E_4C_3$, $C_{10}E_4C_2$, and $C_{11}E_4C_1$, for which a tetrakis(oxyethylene) block (E_4 in $C_kE_4C_{12-k}$) is located at the center to the end of the molecule. The skeletal structural formulas of $C_kE_4C_{12-k}$s ($k = 6-11$) are shown in Figure 1.

Experimental Methods

Materials. All of the compounds studied were synthesized in this work. $C_7E_4C_5$, $C_8E_4C_4$, $C_9E_4C_3$, $C_{10}E_4C_2$, and $C_{11}E_4C_1$ were prepared from pertinent 1-chloroalkanes, where "alkane" corresponds to a longer alkyl group C_k in the synthesized $C_kE_4C_{12-k}$, and tetraethylene glycol monoalkyl ethers, where

* To whom correspondence should be addressed. E-mail: kfuku@sci.hiroshima-u.ac.jp.

10.1021/jp061564d CCC: $33.50
Published on Web 08/01/2006

$C_6E_4C_6$ C–C–C–C–C–C–(**O**–C–C)$_4$–**O**–C–C–C–C–C–C

$C_7E_4C_5$ C–C–C–C–C–C–C–(**O**–C–C)$_4$–**O**–C–C–C–C–C

$C_8E_4C_4$ C–C–C–C–C–C–C–C–(**O**–C–C)$_4$–**O**–C–C–C–C

$C_9E_4C_3$ C–C–C–C–C–C–C–C–C–(**O**–C–C)$_4$–**O**–C–C–C

$C_{10}E_4C_2$ C–C–C–C–C–C–C–C–C–C–(**O**–C–C)$_4$–**O**–C–C

$C_{11}E_4C_1$ C–C–C–C–C–C–C–C–C–C–C–(**O**–C–C)$_4$–**O**–C

Figure 1. Skeletal structural formulas of $C_kE_4C_{12-k}$s ($k = 6-11$).

"monoalkyl" corresponds to a shorter alkyl group C_{12-k}. A phase-transfer catalyst, tetrabutylammonium hydrogensulfate,[18] was used in the synthesis. $C_6E_4C_6$ was prepared by the same method as above from 1-chlorohexane and tetraethylene glycol. All $C_kE_4C_{12-k}$s thus synthesized were purified by repeated vacuum distillations and Kugelrohr distillation. Some of the compounds were purified by column chromatography on silica gel prior to distillation. The purity was checked by gas chromatography to be 99.85% for $C_6E_4C_6$, 99.86% for $C_7E_4C_5$, 99.84% for $C_8E_4C_4$, 99.76% for $C_9E_4C_3$, 99.79% for $C_{10}E_4C_2$, and 99.78% for $C_{11}E_4C_1$.

Infrared Measurements. The infrared spectra of $C_kE_4C_{12-k}$s ($k = 6-11$) were recorded on a Perkin−Elmer Spectrum One spectrometer with a resolution of 2.0 cm^{-1}. A Peltier cryostat cell was used for controlling the temperature of the sample in a range from 230 to 290 K with an accuracy of ±0.2 K. The effect of solidification conditions on the observed spectra was examined by changing the rate of cooling or by annealing the solidified substance. We studied two cooling processes; (1) the liquid sample at room temperature was cooled rapidly with a rate of cooling faster than −20 K min^{-1} and (2) the liquid sample was cooled slowly with a rate of cooling slower than −5 K min^{-1}. Thus, we adopted four different methods of solidification; the liquid substance was rapidly cooled to 230 K without subsequent annealing (method 1), the liquid substance was rapidly cooled to 230 K, and the resultant solidified substance was annealed by warming to a temperature slightly below the melting point and was then cooled to 230 K (method 2), the liquid substance was slowly cooled to 230 K without subsequent annealing (method 3), and the liquid substance was slowly cooled to 230 K and the resultant solidified substance was annealed (method 4).

DSC Measurements. The DSC curves were measured on a Shimadzu DSC-50 differential scanning calorimeter equipped with a Shimadzu LTC-50 cooling jacket. The sample of about 5 mg sealed in a standard aluminum cell was placed in a sample holder under an atmosphere of dry nitrogen flowing at a rate of 30 mL min^{-1} and was solidified at two different rates of cooling, −10.0 and −3.0 K min^{-1}. All samples were kept at about 220 K for 30 min before DSC measurements. Annealing was applied to the solidified samples to examine the thermal-history dependence of the DSC curves. The thermodynamic quantities were derived from the DSC curves measured at a rate of heating of 3.0 K min^{-1} over a temperature range from 230 to 290 K. Measurements at different rates of heating, that is, 0.1, 0.3, 1.0, and 10.0 K min^{-1}, were also performed to examine the possible effects of the scan rate on the DSC curves. The temperature and enthalpy change were calibrated using the standard samples, *n*-dodecane, *n*-hexadecane, and indium. The reproducibility of the observed DSC curves was confirmed by the measurements on different samples of the same compound.

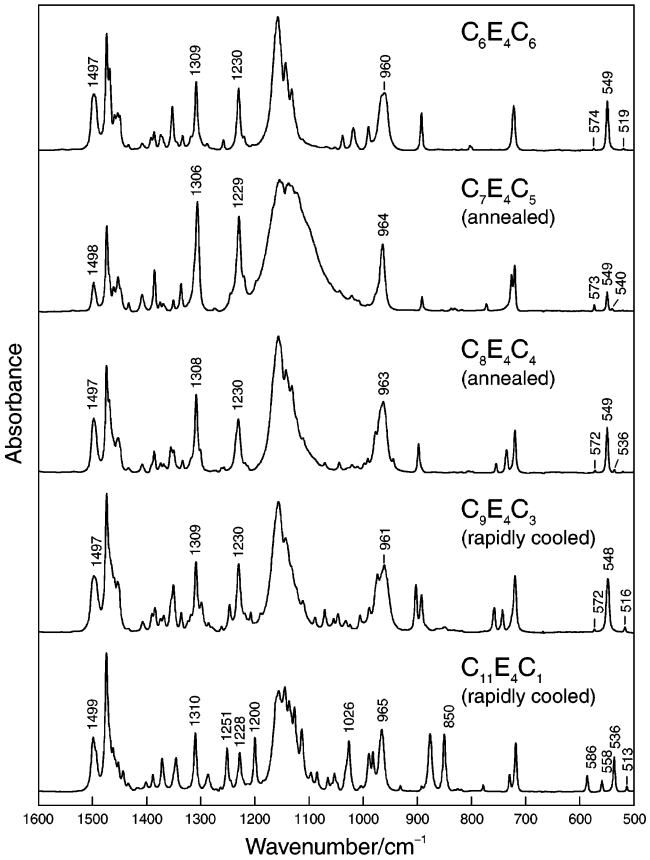

Figure 2. Type-A infrared spectra of $C_kE_4C_{12-k}$s measured at 230 K. The wavenumbers of conformation key bands are indicated in the Figure.

Calculations

Normal coordinate calculations were performed on important molecular forms of $C_kE_4C_{12-k}$s ($k = 6-11$) by using the program MVIB[19] for Windows. The molecular forms were selected by considering the observed infrared bands that are characteristic of particular local conformations and those bands that are strongly affected by the chain length. The calculated results are used for the determination of molecular conformation and the elucidation of vibrational modes.

Results and Discussion

Interpretation of Infrared Spectra. Of the $C_kE_4C_{12-k}$s studied, $C_7E_4C_5$, $C_8E_4C_4$, $C_9E_4C_3$, and $C_{11}E_4C_1$ exhibited two different infrared spectra, depending on the conditions of solidification. The spectra of $C_7E_4C_5$ and $C_8E_4C_4$ obtained by methods 1 and 3 are different from those obtained by methods 2 and 4. The spectra of $C_9E_4C_3$ and $C_{11}E_4C_1$ depend subtly on the solidification conditions. Namely, method 1 gave the spectra different from, but sometimes the same as, those obtained by methods 2, 3, and 4. The occurrence of the different solids by rapid cooling (method 1) for these compounds is most likely associated with a crystallization mechanism that the rate-determining step of melt crystallization is a nucleation process, as will be discussed later. Because the spectrum that is unique to method 1 appears more frequently than the other, we take the unique one as a spectrum of method 1 for $C_9E_4C_3$ and $C_{11}E_4C_1$. $C_6E_4C_6$ and $C_{10}E_4C_2$ each gave the same spectrum irrespective of the solidification conditions.

The infrared spectra of solid $C_kE_4C_{12-k}$s measured at 230 K are classified into two types, A and B, according to their characteristic spectral features. Figures 2 and 3 show the spectra

TABLE 1: Conformation Key Bands of the Alkyl Group Observed for Type-B Spectra of $C_kE_4C_{12-k}$s ($k = 7-11$)

ν_{obs}[a]/cm^{-1}					
$C_7E_4C_5$[b]	$C_8E_4C_4$[b]	$C_9E_4C_3$[c]	$C_{10}E_4C_2$	$C_{11}E_4C_1$[c]	conformational assignment[d]
			814 vw		C_2, OC−C−O−CC in G−T−T
	810 vw				C_4, CO−C−C−CC in T−G−T
			796 vw		C_{10}, CC−C−C−C−C−C−C−C−C−CO in T−T−T−T−T−T−T−G
		782 vw			C_9, CC−C−C−C−C−C−C−CO in T−T−T−T−T−T−G
				777 vw	C_{11}, CC−C−C−C−C−C−C−C−C−CO in T−T−T−T−T−T−T−G
775 vw					C_7, CC−C−C−C−C−CO in T−T−T−G; C_5, OC−C−C−CC in G−T−T
			763 vw		C_{10}, CC−C−C−C−C−C−C−C−C−CO in T−T−T−T−T−T−T−G
		762 vw			C_3, OC−C−O−C−CC in G−T−T−T
	756 vw				C_8, CC−C−C−C−C−C−CO in T−T−T−T−T−G
				750 vw	C_{11}, CC−C−C−C−C−C−C−C−C−CO in T−T−T−T−T−T−T−G
		742 vw			C_9, CC−C−C−C−C−C−C−CO in T−T−T−T−T−T−G
	739 vw				C_4, CO−C−C−CC in T−G−T
			735 vw		C_{10}, CC−C−C−C−C−C−C−C−C−CO in T−T−T−T−T−T−T−G
				730 vw	C_{11}, CC−C−C−C−C−C−C−C−C−CO in T−T−T−T−T−T−T−G
729 w					C_5, OC−C−C−CC in G−T−T
724 w	723 w	716 m	716 m	716 m	all conformations in common

[a] Approximate relative intensities: m, medium; w, weak; vw, very weak. [b] Unannealed. [c] Slowly cooled or annealed. [d] Based on normal coordinate calculations. T, trans; G, gauche.

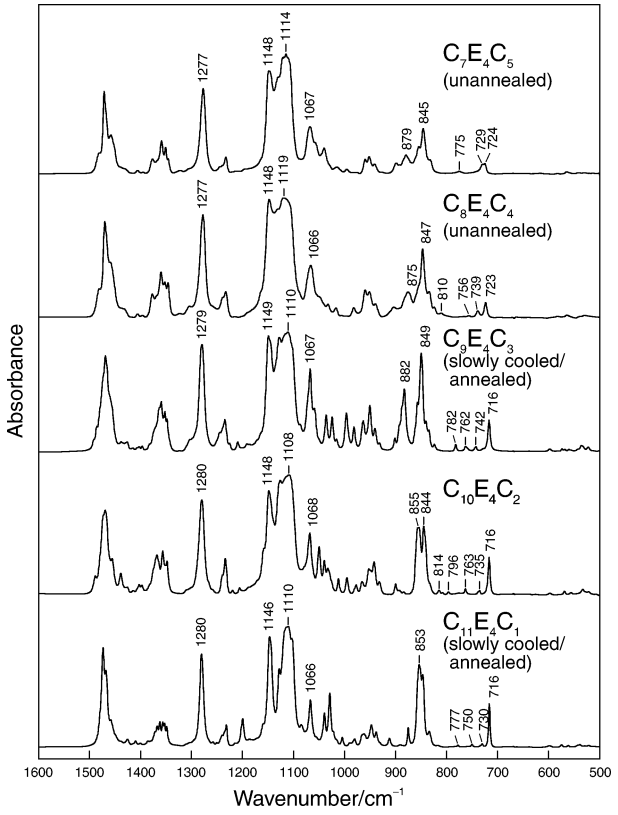

Figure 3. Type-B infrared spectra of $C_kE_4C_{12-k}$s measured at 230 K. The wavenumbers of conformation key bands are indicated in the Figure.

of types A and B, respectively. The characteristic features of the type-A and type-B spectra are essentially the same as those of the same type spectra for $C_nE_mC_n$s studied previously.[15] The type-A spectra show a distinct band at 1500−1495 cm^{-1}, sharp bands at about 1310 and 1230 cm^{-1}, a broad band centered at 965−960 cm^{-1}, and a few bands in the 600−500 cm^{-1} region. The spectra of $C_6E_4C_6$, $C_7E_4C_5$ (annealed), $C_8E_4C_4$ (annealed), $C_9E_4C_3$ (rapidly cooled), and $C_{11}E_4C_1$ (rapidly cooled) are of this type. The spectra of type B are characterized by a well-defined band at about 1280 cm^{-1}, strong broad bands in the 1150−1100 cm^{-1} region, a medium-intensity band at about 1065 cm^{-1}, and a complex spectral feature in the 900−800 cm^{-1} region. The spectra of $C_7E_4C_5$ (unannealed), $C_8E_4C_4$ (unannealed), $C_9E_4C_3$ (slowly cooled or annealed), $C_{10}E_4C_2$, and $C_{11}E_4C_1$ (slowly cooled or annealed) are grouped into this type.

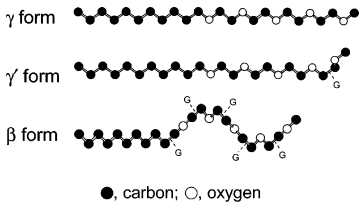

Figure 4. Skeletal models of the $C_kE_4C_{12-k}$ molecule. The models of $C_{11}E_4C_1$ are shown as an illustration. Only the bonds in the gauche conformation are indicated by G; others are in the trans conformation.

Molecular Conformation and Polymorphism. The molecular conformations of $C_kE_4C_{12-k}$s were studied by the combined use of conformation key bands[20−22] and the results of normal coordinate calculations. The type-A spectra of $C_6E_4C_6$, $C_7E_4C_5$ (annealed), $C_8E_4C_4$ (annealed), and $C_9E_4C_3$ (rapidly cooled) closely resemble one another, but the spectrum of $C_{11}E_4C_1$ (rapidly cooled) exhibits several additional bands such as those at 1251, 1200, 1026, and 850 cm^{-1}. The characteristic bands of the type-A spectra for $C_kE_4C_{12-k}$s agree with the bands observed for the γ-form $C_nE_mC_n$s with a planar structure.[15] The bands at 1500−1495, 1310, and 1230 cm^{-1} are assigned to the CH_2 scissoring, wagging, and twisting modes, respectively, of the trans−trans−trans $CH_2O-CH_2-CH_2-OCH_2$ segment in the oligo(oxyethylene) chain.[22] The evaluation of the relevant spectral data proves that the molecular form of $C_kE_4C_{12-k}$s that give the type-A spectra, except $C_{11}E_4C_1$, is the γ form. This structure was confirmed by the normal coordinate calculations. The skeletal molecular model of the γ form is depicted in Figure 4, along with the models of other forms.

The distinctive spectral feature of the rapidly cooled $C_{11}E_4C_1$ reminds us of a molecular form of methoxy-terminated alkyl/oligo(oxyethylene) block compounds, $C_8E_mC_1$ ($m = 1-3$)[23] and $C_{16}E_mC_1$ ($m = 3$ and 4).[17] This molecular form consists of all-trans but gauche conformation in the methoxy-terminated $OCH_2-CH_2OCH_3$ part. The observation of the bands at 1251 and 850 cm^{-1} in the spectrum of $C_{11}E_4C_1$ (rapidly cooled) provides evidence for this particular conformation.[17,23] This conformation is further confirmed by the bands at 1200 and 1026 cm^{-1} arising from the methoxy rocking and the CH_2-O-CH_3 stretching, respectively, of the terminal $OCH_2-CH_2-OCH_3$ part in the gauche−trans conformation. The molecular

TABLE 2: Molecular Forms of $C_kE_4C_{12-k}$s ($k = 6-11$) in the Solid State

	molecular form[a]					
solidification conditions[b]	$C_6E_4C_6$	$C_7E_4C_5$	$C_8E_4C_4$	$C_9E_4C_3$	$C_{10}E_4C_2$	$C_{11}E_4C_1$
unannealed, rapidly cooled[c] (method 1)	γ	β	β	γ	β	γ'
unannealed, slowly cooled[d] (method 3)	γ	β	β	β	β	β
annealed (methods 2 and 4)	γ	γ	γ	β	β	β

[a] For molecular forms, see Figure 4. [b] For the method of solidification given in parentheses, see the text. [c] Rate of cooling faster than -20 K min^{-1}. [d] Rate of cooling slower than -5 K min^{-1}.

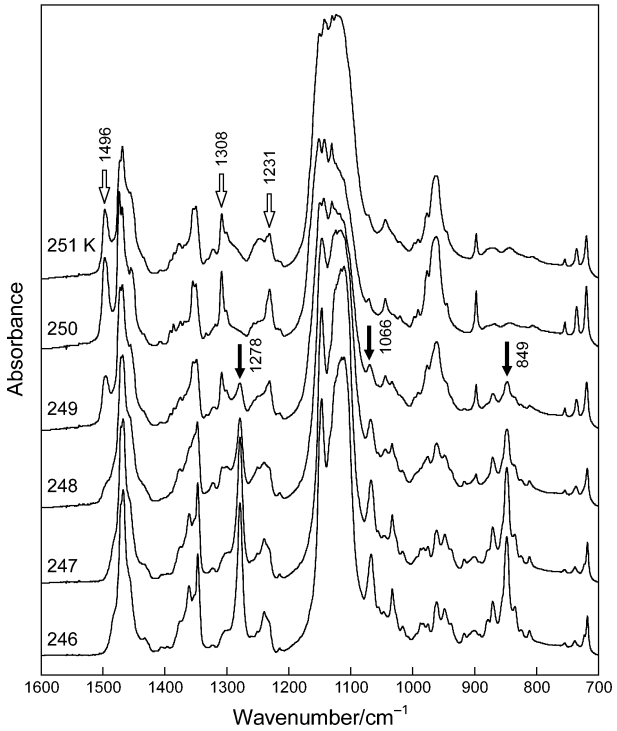

Figure 5. Infrared spectra of $C_8E_4C_4$ in the process of heating the solid obtained by rapid cooling without subsequent annealing. The wavenumbers of conformation key bands (open arrows for type A and filled arrows for type B) are indicated in the Figure.

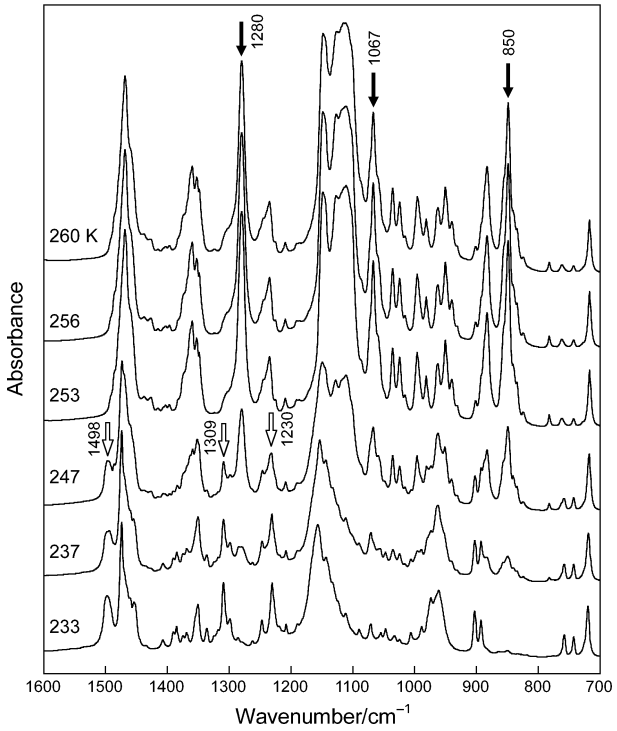

Figure 6. Infrared spectra of $C_9E_4C_3$ in the process of heating the solid obtained by rapid cooling without subsequent annealing. The wavenumbers of conformation key bands (open arrows for type A and filled arrows for type B) are indicated in the Figure.

form of $C_{11}E_4C_1$ (rapidly cooled) is thus determined to be planar but bent at the methoxy terminal. This form, to be called the γ' form, is shown in Figure 4.

In the spectra of type B, the characteristic bands located at about 1280 and 1065 cm^{-1} are associated with the trans−gauche−trans conformation of the O−CH_2−CH_2−O segment in the oligo(oxyethylene) chain.[22] The observation of these bands, supplemented by the absence of key bands for other conformations, leads to a helical structure of the oligo(oxyethylene) block. The conformation of the alkyl blocks was analyzed by normal coordinate calculations on individual molecules, because the vibrational wavenumbers of short alkyl groups are significantly affected not only by the conformational state but also by the chain length. The infrared bands in the 820−700 cm^{-1} region were found to be keys to the conformation of the alkyl group. The relevant conformation key bands for $C_7E_4C_5$ (unannealed), $C_8E_4C_4$ (unannealed), $C_9E_4C_3$ (slowly cooled or annealed), $C_{10}E_4C_2$, and $C_{11}E_4C_1$ (slowly cooled or annealed) are listed in Table 1. The analysis has shown that the alkyl groups in these triblock compounds possess the all-trans conformation but the gauche conformation around the CH_2-CH_2−CH_2O bond adjacent to the tetrakis(oxyethylene) block. Thus, the overall molecular form of the compounds that exhibit the type-B spectra is the β form (Figure 4). In our previous study,[16] we have found another form for $C_8E_4C_4$ in the metastable solid state, namely the $\beta\alpha$ form, for which the conformation of the butoxy terminal OCH_2−CH_2−CH_2CH_3 is trans−trans. Very fast cooling with liquid nitrogen at a rate of about -70 K min^{-1} most probably brought about the occurrence of this molecular form.[16]

The molecular forms of $C_kE_4C_{12-k}$s ($k = 6-11$) in the solid state are summarized in Table 2. The molecular conformation changes with a change of the position of the tetrakis(oxyethylene) block in the molecule, as well as a change of the solidification conditions. The stable molecular form after being annealed is the γ form for $C_6E_4C_6$, $C_7E_4C_5$, and $C_8E_4C_4$, and is the β form for $C_9E_4C_3$, $C_{10}E_4C_2$, and $C_{11}E_4C_1$. This result indicates that the stable molecular form changes from a fully planar structure (γ form) to a planar/helical/planar structure (β form) when the position of the tetrakis(oxyethylene) block changes from the center to the end of the molecule.

As seen in Table 2, $C_7E_4C_5$, $C_8E_4C_4$, $C_9E_4C_3$, and $C_{11}E_4C_1$ exhibit conformational polymorphism depending on the method of solidification. To investigate the conformational transformation with varying temperature, we observed the infrared spectra of these compounds in the process of heating the solid obtained by rapid cooling without annealing. The spectra of $C_8E_4C_4$ and $C_9E_4C_3$ are shown in Figures 5 and 6, respectively. In the spectra of $C_8E_4C_4$, the bands at 1278, 1066, and 849 cm^{-1}, which are characteristic of type B, lose their intensities at higher temperatures, whereas the bands at 1496, 1308, and 1231 cm^{-1},

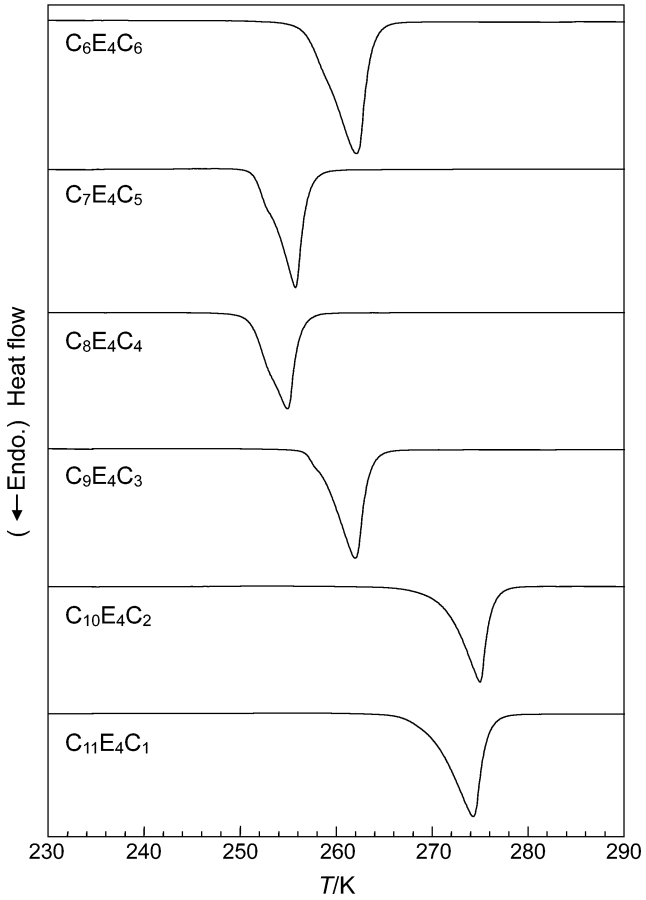

Figure 7. DSC curves for the annealed samples of $C_kE_4C_{12-k}$s (k = 6−11) measured at a rate of heating of 3.0 K min^{-1}.

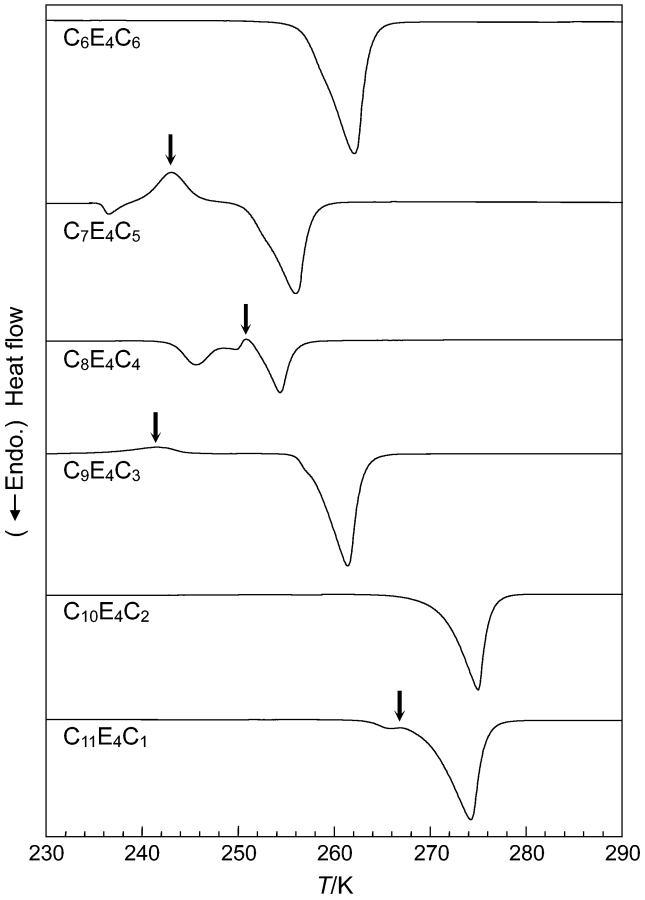

Figure 8. DSC curves for the unannealed samples of $C_kE_4C_{12-k}$s (k = 6−11) measured at a rate of heating of 3.0 K min^{-1}. The arrows indicate the positions of exothermic peaks.

characteristic of type A, increase in their intensities. The spectral change from type B to type A with increasing temperature indicates a conformational transformation from the β form to the γ form. For $C_9E_4C_3$, the spectrum of type A is replaced with the spectrum of type B at higher temperatures, just opposite to what was observed for $C_8E_4C_4$. Accordingly, the conformation of $C_9E_4C_3$ changes from the γ form to the β form. The conformational transformations observed for $C_8E_4C_4$ and $C_9E_4C_3$ were found to be monotropic. The spectral behavior with temperature of $C_7E_4C_5$ is similar to that of $C_8E_4C_4$ (from type B to type A), and the spectral behavior of $C_{11}E_4C_1$ is similar to that of $C_9E_4C_3$ (from type A to type B).

The above consequences indicate that the stable molecular form of $C_7E_4C_5$ and $C_8E_4C_4$ is the γ form and the metastable form is the β form, whereas the stable form of $C_9E_4C_3$ and $C_{11}E_4C_1$ is the β form and the metastable form is the γ form or the γ' form. Although the metastable β form for $C_7E_4C_5$ and $C_8E_4C_4$ conforms to the previous results for other C_nE_m-$C_{n'}$s,[14−16,24,25] the metastable γ or γ' form with a planar oligo(oxyethylene) block is a new finding in the present work.

The conformational polymorphism observed for $C_kE_4C_{12-k}$s can be explained by a crystallization competition between the alkyl and oligo(oxyethylene) blocks with different cross-sectional areas.[15] The $C_nE_mC_{n'}$ triblock compounds adopt either a planar/helical/planar form or a planar form, depending on the relative rates of crystallization in the component blocks. Namely, if the oligo(oxyethylene) block with an intrinsic helical structure crystallizes faster than the alkyl block, then the planar/helical/planar form will be preferentially formed. If, however, the alkyl block crystallizes faster than the oligo(oxyethylene) block, then the alkyl block with a planar structure hinders the formation of a helical oligo(oxyethylene) block. As a result, the planar form will be preferentially formed in this case.

According to the results in Table 2, the oligo(oxyethylene) block seems to crystallize faster than the alkyl block for $C_7E_4C_5$, $C_8E_4C_4$, and $C_{10}E_4C_2$ when the sample is solidified by rapid cooling. The slow cooling, however, promotes faster crystallization of the oligo(oxyethylene) block for all $C_kE_4C_{12-k}$s studied except $C_6E_4C_6$. It is important to note that $C_kE_4C_{12-k}$ molecules in the solid obtained by cooling the liquid assume one single form, either the γ (or γ') form or the β form, but not the admixture of these. This implies that the rate-determining step of melt crystallization of the triblock compounds is a nucleation process. Further information on the nucleation process is necessary to understand the oligo(oxyethylene)-position dependent crystallization competition between the alkyl and oligo(oxyethylene) blocks.

Melting Behavior. The DSC curves for the annealed samples of $C_kE_4C_{12-k}$s (k = 6−11) measured at a rate of heating of 3.0 K min^{-1} are shown in Figure 7, and those for the unannealed samples solidified from the liquid at a rate of cooling of −10.0 K min^{-1} are shown in Figure 8. The curves for the annealed samples (Figure 7) exhibit substantially one single endothermic peak arising from the melting of the stable solid, namely, the γ-form solid for $C_6E_4C_6$, $C_7E_4C_5$, and $C_8E_4C_4$, and the β-form solid for $C_9E_4C_3$, $C_{10}E_4C_2$, and $C_{11}E_4C_1$ (Table 2). In the DSC curves of $C_6E_4C_6$, $C_7E_4C_5$, $C_8E_4C_4$, and $C_9E_4C_3$, an unresolved shoulder is observed at the lower-temperature side of the main peak. Although this shoulder could be assigned to a solid−solid transition, we consider the composite peak for these compounds as a single endothermic peak due to the melting,

TABLE 3: Phase Transitions of Unannealed Samples of $C_kE_4C_{12-k}$s (k = 6−11)

compound	phase transitions[a]						
$C_6E_4C_6$	γ-form solid (stable phase)	258.0 K (endo) ⟶	liquid				
$C_7E_4C_5$	β-form solid (metastable phase)	236.6 K (endo) ⟶	partially melted β-form solid[b] (metastable phase)	≈241 K (exo) ⟶	γ-form solid (stable phase)	252.8 K (endo) ⟶	liquid
$C_8E_4C_4$	β-form solid (metastable phase)	243.9 K (endo) ⟶	partially melted β-form solid[b] (metastable phase)	≈250 K (exo) ⟶	γ-form solid (stable phase)	251.8 K (endo) ⟶	liquid
$C_9E_4C_3$	γ-form solid (metastable phase)	≈240 K (exo) ⟶	β-form solid (stable phase)	258.8 K (endo) ⟶	liquid		
$C_{10}E_4C_2$	β-form solid (stable phase)	270.7 K (endo) ⟶	liquid				
$C_{11}E_4C_1$[c]	γ′-form solid (metastable phase)	≈264 K (endo) ⟶	liquid (metastable)	≈266 K (exo) ⟶	β-form solid (stable phase)	269.9 K (endo) ⟶	liquid

[a] Transition temperatures are shown above the arrows. Endothermic and exothermic processes are denoted by endo and exo, respectively, in parentheses. [b] Alkyl blocks are melted. [c] The melting behavior of $C_{11}E_4C_1$ is complicated. The melting process shown is the most likely one.

TABLE 4: Thermodynamic Quantities[a] of Stable Solid of $C_kE_4C_{12-k}$s ($k = 6-11$)

	γ-form solid			β-form solid		
	$C_6E_4C_6$	$C_7E_4C_5$	$C_8E_4C_4$	$C_9E_4C_3$	$C_{10}E_4C_2$	$C_{11}E_4C_1$
T_m[b]/K	258.0	252.8	251.8	258.8	270.7(0.1)	269.9(0.3)
ΔH_m/kJ mol^{-1}	59.31(0.16)	55.39(0.45)	54.21(0.33)	55.97(0.38)	62.36(0.24)	61.92(0.10)
ΔS_m[c]/J K^{-1} mol^{-1}	229.9(0.6)	219.1(1.8)	215.3(1.4)	216.3(1.5)	230.3(0.9)	229.5(0.6)

[a] T_m, melting point; ΔH_m, enthalpy of melting; ΔS_m, entropy of melting. Standard deviations are given in parentheses. [b] Standard deviations less than 0.1 K are not shown. [c] $\Delta S_m = \Delta H_m/T_m$.

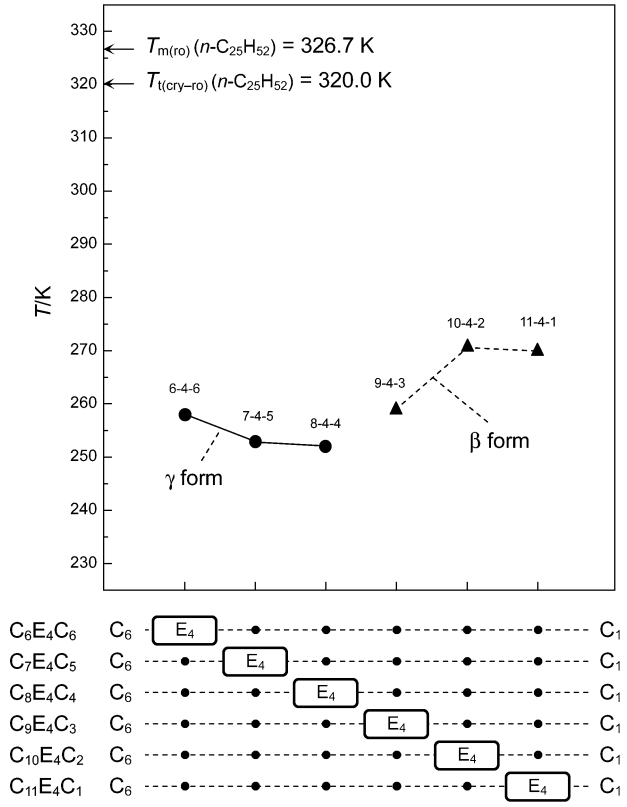

Figure 9. T_m of $C_kE_4C_{12-k}$s ($k = 6-11$), and $T_{m(ro)}$ and $T_{t(cry-ro)}$ of n-$C_{25}H_{52}$.[26] $C_kE_4C_{12-k}$ is denoted as k-4-(12−k).

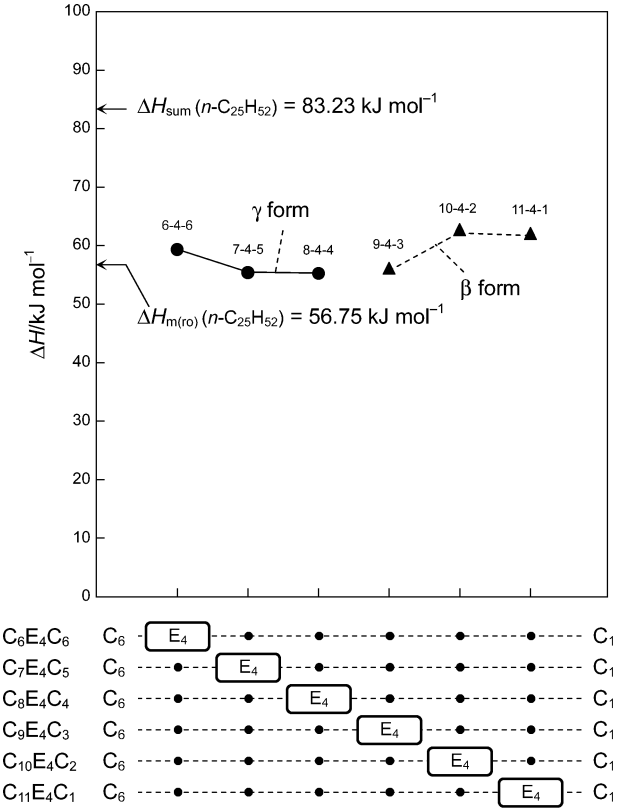

Figure 10. ΔH_m of $C_kE_4C_{12-k}$s ($k = 6-11$), and $\Delta H_{m(ro)}$ and ΔH_{sum} of n-$C_{25}H_{52}$.[26] $C_kE_4C_{12-k}$ is denoted as k-4-(12−k).

because we were unable to separate the shoulder from the main peak even at the slowest rate of heating of 0.1 K min^{-1}. The melting point (T_m) of the stable solid is taken at an extrapolated onset of the endothermic peak, and the entropy of melting (ΔS_m) is expressed as the enthalpy of melting (ΔH_m) divided by T_m.

The DSC curves for the unannealed samples (Figure 8) exhibit a main endothermic peak and, for some of the compounds, an additional weaker endothermic peak at a lower temperature and an exothermic peak as indicated by an arrow in the figure. The melting behavior of $C_6E_4C_6$ and $C_{10}E_4C_2$, which gives only the main endothermic peak, is the same as that for the annealed samples of the same compounds. $C_7E_4C_5$ and $C_8E_4C_4$ show a weak endothermic peak due to the melting of the alkyl blocks in the metastable β-form solid. A similar phase transition has been observed for $C_6E_5C_6$ (unannealed), $C_6E_6C_6$, and $C_6E_7C_6$.[24] The subsequent exothermic process for $C_7E_4C_5$ and $C_8E_4C_4$ is a transition to the stable γ-form solid. The temperature-dependent infrared spectra of $C_8E_4C_4$ (Figure 5) in fact change noticeably from type B (β form) to type A (γ form) in a small temperature range coinciding with the exothermic phase transition. The transition temperature for the main endothermic peak that appears after the exothermic process coincides with the temperature for the endothermic peak (melting point) of the corresponding annealed samples. For $C_9E_4C_3$ and $C_{11}E_4C_1$, the metastable γ-form or γ'-form solid transforms into the stable β-form solid before melting. The phase transitions of the unannealed samples of $C_kE_4C_{12-k}$s ($k = 6-11$) are summarized in Table 3.

The thermodynamic quantities of the stable solid of $C_kE_4C_{12-k}$s ($k = 6-11$) derived from the DSC measurements are listed in Table 4. The dependence of the melting point, T_m, on the position of the tetrakis(oxyethylene) block is shown in Figure 9, where the melting point of the rotator phase ($T_{m(ro)}$) and the crystalline−rotator phase transition temperature ($T_{t(cry-ro)}$) for n-pentacosane (n-$C_{25}H_{52}$)[26] are also shown. The data for n-$C_{25}H_{52}$ will be discussed later in view of the fact that the molecules of $C_kE_4C_{12-k}$s and n-$C_{25}H_{52}$ contain the same number (25) of backbone atoms. The abscissa in Figure 9 and the subsequent two figures indicates the position of the tetrakis-(oxyethylene) block in the molecule. Figure 10 shows the enthalpy of melting, ΔH_m, for $C_kE_4C_{12-k}$s, along with the pertinent data for n-$C_{25}H_{52}$,[26] that is, the enthalpy of melting of the rotator phase ($\Delta H_{m(ro)}$) and a sum (ΔH_{sum}) of $\Delta H_{m(ro)}$ and the enthalpy of crystalline−rotator phase transition. The entropy of melting, ΔS_m, for $C_kE_4C_{12-k}$s is shown in Figure 11, where, again, the data for n-$C_{25}H_{52}$[26] are provided, which include the entropy of melting of the rotator phase ($\Delta S_{m(ro)}$) and a sum (ΔS_{sum}) of $\Delta S_{m(ro)}$ and the entropy of crystalline−rotator phase transition.

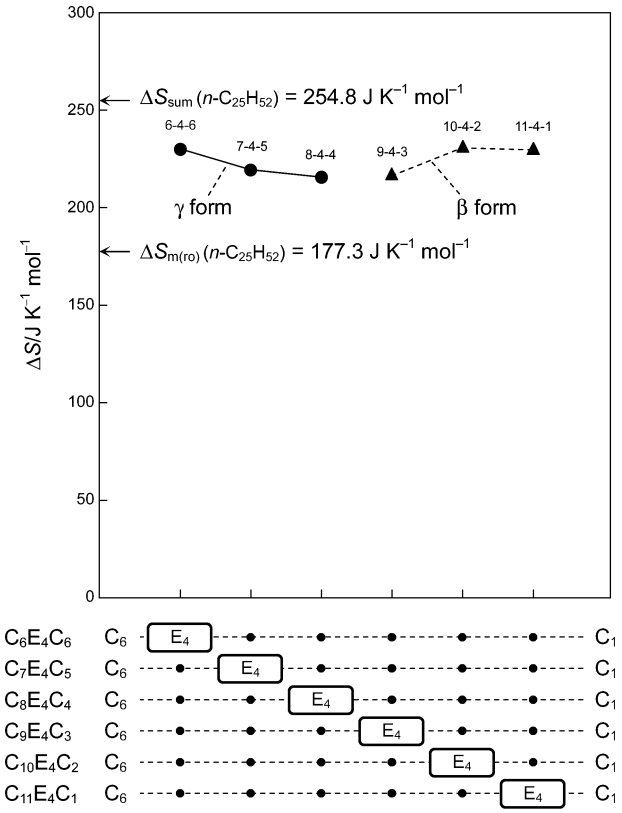

Figure 11. ΔS_m of $C_kE_4C_{12-k}$s ($k = 6-11$), and $\Delta S_{m(ro)}$ and ΔS_{sum} of n-$C_{25}H_{52}$.[26] $C_kE_4C_{12-k}$ is denoted as k-4-($12-k$).

As seen in Figure 9, the values of T_m for $C_kE_4C_{12-k}$s are much lower than the values of $T_{m(ro)}$ and $T_{t(cry-ro)}$ for n-$C_{25}H_{52}$. This observation agrees with our previous findings for analogous triblock compounds.[24,25,27] We have interpreted the lower melting points of the γ-form $C_nE_mC_n$s as due to the higher Gibbs energy of crystal arising from intermolecular repulsive interactions, the conformational restoring force acting in the central oligo(oxyethylene) block, and the electrostatic interaction between ether oxygen atoms.[24,25] This elucidation is confirmed in this work by the fact that the values of ΔH_m for the γ-form $C_kE_4C_{12-k}$s ($k = 6-8$) are about 30% smaller than the value of ΔH_{sum} for n-$C_{25}H_{52}$, and the values of ΔS_m for the γ-form $C_kE_4C_{12-k}$s are only about 10% smaller than the value of ΔS_{sum} for n-$C_{25}H_{52}$. We used here ΔH_{sum} and ΔS_{sum}, rather than $\Delta H_{m(ro)}$ and $\Delta S_{m(ro)}$, for n-$C_{25}H_{52}$, because the stable solid of this compound melts via the rotator phase.[26]

Stabilities of Molecular Forms. Figure 9 shows that, with changing the position of the tetrakis(oxyethylene) block from the center to the end of the molecule, the values of T_m for the γ-form solid decrease, while the values for the β-form solid increase, although $C_{11}E_4C_1$ with the tetrakis(oxyethylene) block at the end of the molecule gives rather a low value. This behavior of the melting point indicates that the γ form is less stabilized, while the β form is more stabilized, with a shift of the tetrakis(oxyethylene) block toward the terminal of the molecule. This result agrees with the stabilities of the molecular forms derived from the spectral analysis (Table 2).

We can explain the present experimental results by the relative stabilities of partial crystal lattices formed by the component blocks. This elucidation is based on an idea that, if the end blocks have a structure of crystal lattices different from that of the central block, then they will destabilize the crystal lattice of the central block. When the tetrakis(oxyethylene) block is located at the center of the $C_kE_4C_{12-k}$ molecule, the end alkyl blocks with considerable lengths can form stable crystal lattices with a planar structure, and their stability, which prevails over the stability of the crystal lattice of the tetrakis(oxyethylene) block, makes the γ form with a planar structure more stable and the β form containing a helical structure less stable. When the tetrakis(oxyethylene) block shifts toward the terminal of the molecule with progressive shortening of one of the alkyl blocks, the crystal lattice formed by practically one available alkyl block is no longer effective in stabilizing the γ form. The decreased stability of the γ form ultimately results in a higher stability of the β form. The lowering of the melting points for the γ-form solid in going from $C_6E_4C_6$ to $C_8E_4C_4$ and the increasing of the melting points for the β-form solid in going from $C_9E_4C_3$ to $C_{10}E_4C_2$ conform to the above explanation.

The values of ΔH_m for $C_kE_4C_{12-k}$s are close to the value of $\Delta H_{m(ro)}$ for n-$C_{25}H_{52}$ (Figure 10). As pointed out in our previous studies,[24,25] the planar structure of the oligo(oxyethylene) block in the γ-form solid is stabilized by the force of a magnitude that maintains the rotator phase of n-alkanes. If the values of ΔH_m for $C_kE_4C_{12-k}$s are lower than the value of $\Delta H_{m(ro)}$ for n-$C_{25}H_{52}$, then the planar structure of the oligo(oxyethylene) block is not stabilized, and the β form in turn becomes more stable. The decrease of the ΔH_m values in going from $C_6E_4C_6$ to $C_8E_4C_4$ is an indication of the conformational transformation from the γ form to the β form at $k = 9$.

Conclusions

In this work, we have studied the effect of the position of an oligo(oxyethylene) block in the molecule on the conformation and melting behavior of $C_kE_4C_{12-k}$ position isomers. The analysis of infrared spectra has revealed that the stable molecular form changes from a fully planar structure (γ form) to a planar/helical/planar structure (β form) with a change of the position of the tetrakis(oxyethylene) block from the center to the end of the molecule. The DSC measurements have shown that the melting points of the γ-form solid decrease and the melting points of the β-form solid increase with a shift of the tetrakis(oxyethylene) block toward the terminal of the molecule. The stabilities of the two molecular forms change over between $k = 8$ and 9. $C_8E_4C_4$ and $C_9E_4C_3$ exhibit contrasting conformational behavior with temperature; when the temperature is increased, the metastable β form of $C_8E_4C_4$ transforms into the stable γ form, while the metastable γ form of $C_9E_4C_3$ transforms into the stable β form. The experimental results of the stabilities of molecular forms are explained by the relative stabilities of partial crystal lattices formed by the alkyl and oligo(oxyethylene) blocks.

The present study has demonstrated the importance of joint research by infrared spectroscopy (vibrational spectroscopy) and calorimetric analysis for clarifying the structural stabilities of block compounds. The findings therefrom will be applied to precise morphological analysis of crystalline block copolymers.

Acknowledgment. This work was partially supported by a Grant-in-Aid for Scientific Research No. 13640513 from the Ministry of Education, Culture, Sports, Science, and Technology (MEXT) of Japan. We thank Mr. Takahiro Mizawa for his assistance in the experiment.

References and Notes

(1) Fujiwara, T.; Miyamoto, M.; Kimura, Y.; Iwata, T.; Doi, Y. *Macromolecules* **2001**, *34*, 4043−4050.

(2) Park, C.; Yoon, J.; Thomas, E. L. *Polymer* **2003**, *44*, 6725−6760.

(3) Sun, L.; Liu, Y.; Zhu, L.; Hsiao, B. S.; Avila-Orta, C. A. *Polymer* **2004**, *45*, 8181−8193.

(4) Bunn, C. W. *Trans. Faraday Soc*. **1939**, *35*, 482−491.
(5) Takahashi, Y.; Tadokoro, H. *Macromolecules* **1973**, *6*, 672−675.
(6) Domszy, R. C.; Booth, C. *Makromol. Chem*. **1982**, *183*, 1051−1070.
(7) Teo, H. H.; Swales, T. G. E.; Domszy, R. C.; Heatley, F.; Booth, C. *Makromol. Chem*. **1983**, *184*, 861−877.
(8) Swales, T. G. E.; Teo, H. H.; Domszy, R. C.; Viras, K.; King, T. A.; Booth, C. *J. Polym. Sci., Polym. Phys. Ed*. **1983**, *21*, 1501−1511.
(9) Yeates, S. G.; Teo, H. H.; Booth, C. *Makromol. Chem*. **1984**, *185*, 2475−2488.
(10) Swales, T. G. E.; Domszy, R. C.; Beddoes, R. L.; Price, C.; Booth, C. *J. Polym. Sci., Polym. Phys. Ed*. **1985**, *23*, 1585−1595.
(11) Swales, T. G. E.; Beddoes, R. L.; Price, C.; Booth, C. *Eur. Polym. J*. **1985**, *21*, 629−634.
(12) Matsuura, H.; Fukuhara, K.; Hiraoka, O. *J. Mol. Struct*. **1988**, *189*, 249−256.
(13) Fukuhara, K.; Sagawa, T.; Kihara, S.; Matsuura, H. *J. Mol. Struct*. **1996**, *379*, 197−204.
(14) Fukuhara, K.; Sakogawa, F.; Matsuura, H. *J. Mol. Struct*. **1997**, *405*, 123−131.
(15) Fukuhara, K.; Hashiwata, K.; Takayama, K.; Matsuura, H. *J. Mol. Struct*. **2000**, *523*, 269−280.
(16) Fukuhara, K.; Masatoki, S.; Yonemitsu, T.; Matsuura, H. *J. Mol. Struct*. **1998**, *444*, 69−76.
(17) Masatoki, S.; Matsuura, H. *J. Chem. Soc., Faraday Trans*. **1994**, *90*, 2769−2774.
(18) Gibson, T. *J. Org. Chem*. **1980**, *45*, 1095−1098.
(19) Matsuura, H. *Comput. Chem*. **1990**, *14*, 59−67.
(20) Zerbi, G.; Magni, R.; Gussoni, M.; Holland-Moritz, K.; Bigotto, A.; Dirlikov, S. *J. Chem. Phys*. **1981**, *75*, 3175−3194.
(21) Maroncelli, M.; Qi, S. P.; Strauss, H. L.; Snyder, R. G. *J. Am. Chem. Soc*. **1982**, *104*, 6237−6247.
(22) Matsuura, H.; Fukuhara, K. *J. Polym. Sci., Part B, Polym. Phys*. **1986**, *24*, 1383−1400.
(23) Masatoki, S.; Matsuura, H.; Fukuhara, K. *J. Raman Spectrosc*. **1994**, *25*, 641−645.
(24) Fukuhara, K.; Mizawa, T.; Inoue, T.; Kumamoto, H.; Matsuura, H. *J. Phys. Chem. B* **2004**, *108*, 515−522.
(25) Fukuhara, K.; Mizawa, T.; Inoue, T.; Kumamoto, H.; Terai, Y.; Matsuura, H.; Viras, K. *Phys. Chem. Chem. Phys*. **2005**, *7*, 1457−1463.
(26) Domalski, E. S.; Hearing, E. D. *J. Phys. Chem. Ref. Data* **1996**, *25*, 1−523.
(27) Fukuhara, K.; Akisue, M.; Matsuura, H. *Chem. Lett*. **2001**, *30*, 828−829.